Molecular engineering of conotoxins: The importance of loop size to alpha-conotoxin structure and function

ARTICLE *in* JOURNAL OF MEDICINAL CHEMISTRY · SEPTEMBER 2008

Impact Factor: 5.45 · Source: OAI

Molecular Engineering of Conotoxins: The Importance of Loop Size to α-Conotoxin Structure and Function

Ai-Hua Jin,[§] Norelle L. Daly,[§] Simon T. Nevin,[†] Ching-I A. Wang,[§] Sebastien Dutertre,[§] Richard J. Lewis,[§] David J. Adams,[†] David J. Craik,[§] and Paul F. Alewood*[,§]

Institute for Molecular Bioscience, and Queensland Brain Institute and School of Biomedical Sciences, University of Queensland, Brisbane, QLD 4072 Australia

Received March 13, 2008

α-Conotoxins are competitive antagonists of nicotinic acetylcholine receptors (nAChRs). The majority of currently characterized α-conotoxins have a 4/7 loop size, and the major features of neuronal α-conotoxins include a globular disulfide connectivity and a helical structure centered around the third of their four cysteine residues. In this study, a novel "molecular pruning" approach was undertaken to define the relationship between loop size, structure, and function of α-conotoxins. This involved the systematic truncation of the second loop in the α-conotoxin [A10L]PnIA [4/7], a potent antagonist of the α7 nAChR. The penalty for truncation was found to be decreased conformational stability and increased susceptibility to disulfide bond scrambling. Truncation down to 4/4[A10L]PnIA maintained helicity and did not significantly reduce electrophysiological activity at α7 nAChRs, whereas 4/3[A10L]PnIA lost both α7 nAChR activity and helicity. In contrast, all truncated analogues lost ∼100-fold affinity at the AChBP, a model protein for the extracellular domain of the nAChR. Docking simulations identified several hydrogen bonds lost upon truncation that provide an explanation for the reduced affinities observed at the α7 nAChR and AChBP.

Introduction

Nicotinic acetylcholine receptors (nAChRs[a]) belong to the family of cysteine-loop ligand-gated ion channels and are involved in many functional roles, including memory, learning, anxiety, and pain.[1,2] Many diseases, including schizophrenia and epilepsy, can be caused by functional defects of nicotinic receptors.[3] As a group of ligands that target muscle and neuronal nAChRs, α-conotoxins have been of interest since the 1980s[4,5] for their remarkable ability to dissect the role of individual subunits of nAChRs.[6−12] Among the more than 20 currently known α-conotoxins,[13] more than half contain a 4/7 loop configuration, with the nomenclature referring to the number of residues in the two "loops" in the backbone, i.e., four in the first loop and seven in the second loop. Figure 1 shows some representative α-conotoxins and their loop spacings. Less common loop sizes include one example of 4/6 (AuIB),[14] three examples of 4/3 (ImI/ImII/RgIA[8,15,16]), one 4/5 example (Pu1.3),[17] and one 4/4 example (BuIA).[18] Structures of native 4/7, 4/6, and 4/3 loop-sized α-conotoxins have been determined by either NMR or crystallography. All α-conotoxin structures show a well-defined consensus structural motif of a helical region centered around the third cysteine residue.[19] Interestingly, the 4/4 globular BuIA showed multiple conformations in solution, including conformers distinct from the native α-conotoxin consensus motif.[20] The discovery of the multiconformational nature of globular BuIA provided a first insight into the influence of loop size on structural integrity of globular α-conotoxins.

In the present study, we investigated whether α-conotoxins with a 4/7 loop size have a structure/function advantage over

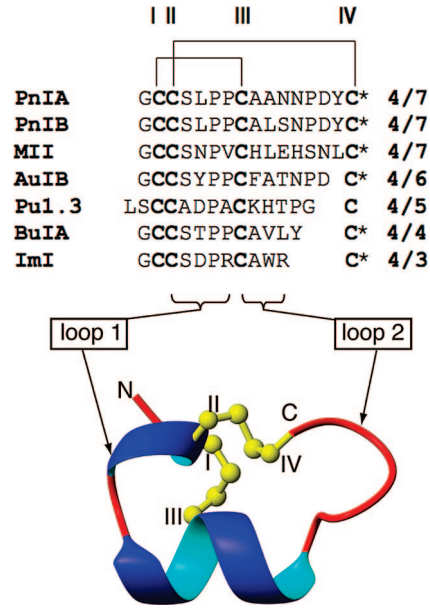

Figure 1. Sequences of selected α-conotoxins with different loop spacings. The amidated C-termini are indicated with asterisks and the disulfide bonded cysteine residues connected with lines. The structure of PnIA (PDB ID code 1PEN) is shown at the bottom of the figure with the cysteine residues shown in ball and stick format and labeled with Roman numerals.

* To whom correspondence should be addressed. Phone: 61 7 3346 2982. Fax: 61 7 3346 2101. E-mail: p.alewood@imb.uq.edu.au.
[§] Institute for Molecular Bioscience.
[†] Queensland Brain Institute and School of Biomedical Sciences.

[a] Abbreviations: ACh, acetylcholine; nAChR, nicotinic acetylcholine receptor; AChBP, acetylcholine binding protein; Ls-AChBP, *Lymnaea stagnalis* acetylcholine binding protein; Ac-AChBP, *Aplysia california* acetylcholine binding protein; Acm, acetamidomethyl; Boc, *tert*-butoxycarbonyl; CD, circular dichroism; DCM, dichloromethane; DIEA, diisopropylethylamine; DQF-COSY, double quantum filtered correlation spectroscopy; ECOSY, exclusive correlation spectroscopy; HBTU, 2-(1*H*-benzotriazole-1-yl)-1,1,3,3-tetramethyluronium hexafluorophosphate; HEPES, *N*-[2-hydroxyethyl]piperazine-*N*′-[2-ethanesulfonic acid]; HF, hydrogen fluoride; HPLC, high performance liquid chromatography; ^{125}I-Bgt, iodine-125 labeled α-bungarotoxin; MBHA, 4-methylbenzhydrylamine; MS, mass spectrometry; NMR, nuclear magnetic resonance; NOESY, nuclear Overhauser spectroscopy; RP-HPLC, reversed-phase high performance liquid chromatography; SEM, standard error of the mean; TFA, trifluoroacetic acid; TFE, trifluoroethanol; TOCSY, total correlation spectroscopy.

10.1021/jm800278k CCC: $40.75
Published on Web 08/28/2008

Table 1. Structural Determinants of α-Conotoxin [A10L]PnIA Affinity for nAChRs[a]

		structural or functional determinants of [A10L]PnIA binding and activity																
exptl strategies	receptor	loop1							loop2									ref
electrophysiology[b]	hα7/r5HT-3 in 293 HEK	G	C	C	**S**	**L**	**P**	**P**	C	**A**	**L**	S	N	P	D	Y	C	21
electrophysiology[b]	Chick α7 in oocytes	G	C	C	S	**L**	**P**	**P**	C	A	**L**	**N**	**N**	**P**	D	**Y**	C	22
X-ray crystallography[b]	Ac-AChBP	**G**	**C**	C	**S**	**L**	**P**	**P**	**C**	**A**	**L**	**N**	**N**	**P**	K	**Y**	C	23
computational docking[b]	α7 nAChR model	G	C	C	S	**L**	**P**	**P**	C	**A**	**L**	N	N	**P**	D	Y	C	29
		G	C	C	S	**L**	**P**	**P**	C	**A**	**L**	N	N	P	**D**	Y	C	23

[a] Residues crucial for affinity on nAChRs, AChBP, and nAChR model are in boldface. [b] In electrophysiological studies, position and alanine scanning mutants were used and compared in determining the potency. In X-ray crystallography and computational docking studies, the distances between residues of mutant PnIA bound to the receptor were measured and analyzed.

Table 2. Sequences of Loop II Truncated [A10L]PnIA Analogues[a]

peptides	pruned sequences																
[A10L]PnIA	G	C	C	S	L	P	P	C	**A**	**L**	**N**	**N**	**P**	**D**	***Y*** ×	C
4/6[A10L]PnIA	G	C	C	S	L	P	P	C	**A**	**L**	**N**	**N**	**P**	***D*** ×		C
4/5[A10L]PnIA	G	C	C	S	L	P	P	C	**A**	**L**	**N**	**N**	***P*** ×			C
4/4[A10L]PnIA	G	C	C	S	L	P	P	C	**A**	**L**	**N**	***N*** ×				C
4/3[A10L]PnIA	G	C	C	S	L	P	P	C	**A**	**L**	**N**					C

[a] The loop II (C-terminal loop) residues are in boldface. × highlights pruned residues. Note: The disulfide bond connectivity for all of these peptides is CysI−III and CysII−IV.

other loop sizes and determined how loop size affects the structural integrity and function of α-conotoxins. The 4/7 conotoxin [A10L]PnIA was chosen as the model α-conotoxin to probe these questions, as it is the most potent known α7-selective conotoxin. Moreover, the role of individual amino acids on the affinity of the closely related conotoxins PnIB, [A10L]PnIA, and the double mutant [A10L, D14K]PnIA for homologous α7 nAChRs (including a molluscan binding protein, AChBP, and an α7 nAChR model) has been widely investigated[10,21−23] (Table 1). Furthermore, the structures of native PnIA and PnIB have been well characterized.[24,25] In this paper, we report the chemical synthesis, structure, and activity of truncated or "pruned" analogues (i.e., 4/6, 4/5, 4/4, and 4/3 versions, Table 2) of [A10L]PnIA. Our data indicate that the 4/4, 4/5, and 4/6[A10L]PnIA truncated analogues maintain almost full potency on rat α7 nAChRs expressed in oocytes, whereas 4/3[A10L]PnIA is inactive. NMR and CD data showed that "pruning" loop 2 of [A10L]PnIA from seven to three amino acids leads to a gradual loss of helical structure, with complete loss of structure being observed for the 4/3 analogue, despite it possessing the same loop sizes as several known helical 4/3 α-conotoxins.

Results

Rational Design of the Truncated Peptides. Mutagenesis studies on α-conotoxins (i.e., ImI, MII, PnIA/PnIB) have revealed that the important binding residues comprise several residues in the first loop and one or two residues in the second loop.[10,26,27] Cocrystal structures of molluscan ACh binding protein (AChBP) with α-conotoxins show that the active conformation of α-conotoxins maintains a helical structure.[23,28] Docking studies by Dutertre et al.[29] showed that P6 in the first loop acts as an anchor for α-conotoxins to the AChBP and additional contacts strengthen the interaction. Given this understanding, we investigated whether helical structure is essential for the activity of neuronally active α-conotoxins. Using a "molecular pruning" strategy, a term coined by Andrews et al.[30] to describe the trimming of superfluous foliage from an active molecule to simplify the structure and/or promote activity, we investigated the highly potent and helical conotoxin [A10L]PnIA where the role of residues in the second loop was contentious. Previous AChBP crystallography and related nAChR modeling studies revealed van der Waals interactions between Tyr15 of [A10L]PnIA and Cys188 and close contacts between Pro13 of [A10L]PnIA and Arg57 on the Ac-AChBP subunit. A hydrogen bond has also been predicted between Asp14 of [A10L]PnIA and Lys75 in a nAChR model.[23] In contrast, mutagenesis studies have indicated that proline substitutions at position 13 (Pro → Hyp), neutralization of the negative charge at position 14 (Asp → Asn), or removal of the aromatic ring and hydroxyl moiety at position 15 (Tyr → Ala) had little effect on the binding affinity.[21] Since the native 4/7 and 4/3 α-conotoxins have helical structures, we proposed that pruned shorter versions of [A10L]PnIA could maintain full potency provided that significant structural integrity could be maintained. The "pruned" molecules comprised truncated loop 2 analogues as shown in Table 2.

Peptide Synthesis. Construction of the peptide chain of truncated [A10L]PnIA analogues was achieved by standard manual Boc-based solid phase peptide synthesis starting from MBHA resin. The crude samples after cleavage gave one single main peak for all peptides, and the observed mass matched the calculated mass. The first pair of cysteine residues was linked by treatment with 0.1 M NH_4HCO_3 overnight, and the second disulfide bond was formed by iodine oxidation. Two-step deprotection and oxidation for selective synthesis of these unnatural conotoxins was sufficient to generate a single globular isomer for each peptide. All peptides have an observed mass matching the calculated mass. Figure 2 shows the HPLC and MS profiles of the final truncated peptides. An additional peptide 4/3[P7R, A10L]PnIA was synthesized by the same method and its HPLC and MS profile is in Supporting Information Figure 1.

Electrophysiological Assay of [A10L]PnIA Analogues on Rat α7 nAChR Receptors Expressed in *Xenopus* Oocytes. Oocytes were isolated from *Xenopus laevis*, and rat α7 nAChR RNA was injected and expressed. The effect of the truncated [A10L]PnIA peptides on rat α7 nAChRs expressed in *Xenopus* oocytes was determined. Membrane currents were evoked with 200 μM ACh with the oocytes voltage clamped at −80 mV. Concentration−response curves were used to compare the relationship of each analogue with the 4/7 control, [A10L]PnIA. A summary of the IC_{50} values is presented in Table 3. [A10L]PnIA inhibited the ACh-induced current with an IC_{50} value of 55 ± 9 nM (n = 6). Truncated 4/4, 4/5, and 4/6[A10L]PnIA maintained similar potency to [A10L]PnIA with IC_{50} values of 207 ± 66 nM (n = 10), 79 ± 13 nM (n = 8), and 115 ± 45 nM (n = 8), respectively. 4/3[A10L]PnIA did not inhibit the peak ACh-evoked current amplitude at concentrations up to 1 μM (n = 8). Concentration−response curves for the [A10L]PnIA analogues were generated from six different concentrations of inhibitor, and results are shown in Figure 3. In addition, the position 7 mutant 4/3[P7R, A10L]PnIA behaved

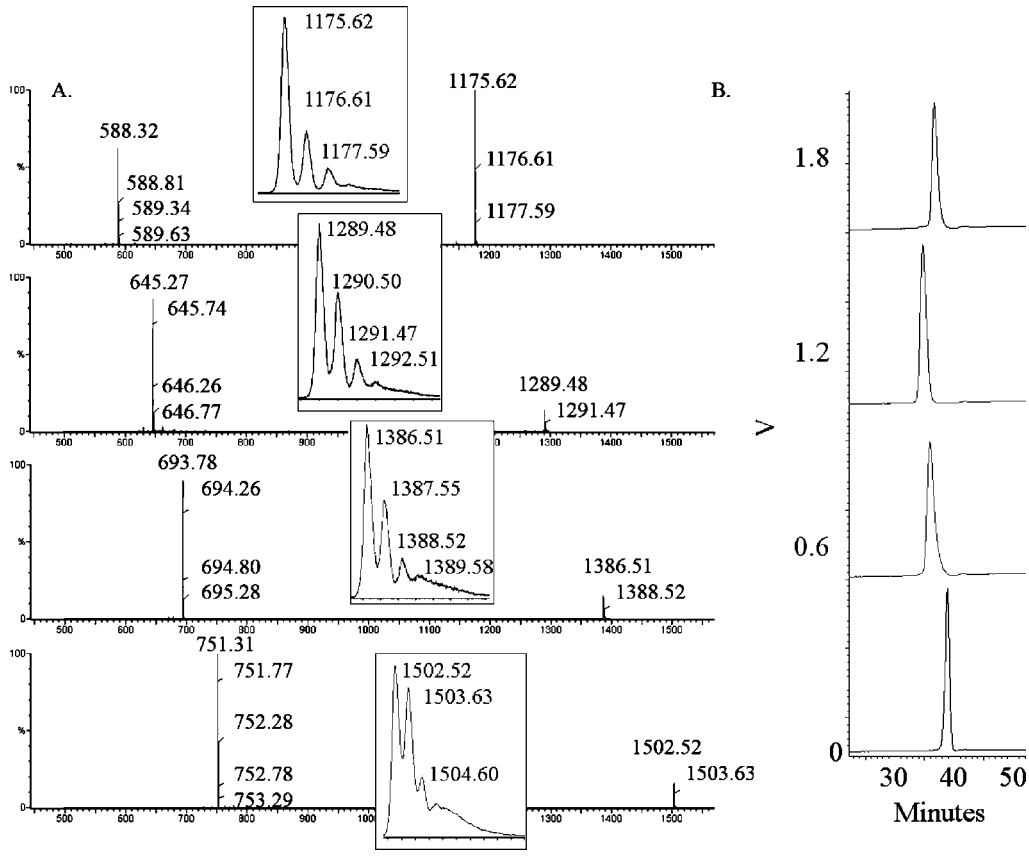

Figure 2. MS and HPLC profiles of purified products of truncated peptides. (A) Mass spectra top to bottom are for 4/3, 4/4, 4/5, and 4/6[A10L]PnIA, respectively. The M + H ions are amplified and shown in the inserted box. The calculated monoisotopic masses top to bottom are 1174.44, 1288.48, 1385.53, and 1501.57 Da, and the observed monoisotopic masses top to bottom are 1174.64, 1288.54, 1385.51, and 1501.52 Da, respectively. (B) HPLC traces top to bottom are 4/3, 4/4, 4/5, and 4/6[A10L]PnIA, respectively.

Table 3. Potency of PnIA, [A10L]PnIA, and Truncated [A10L]PnIA Analogues at Rat α7 nAChRs and Ls-AChBP

[A10L]PnIA analogues	α7 nAChR, IC_{50} ± SEM (nM), electrophysiology	Ls-AChBP, K_i (CI) (nM), ^{125}I-Bgt binding
[A10L]PnIA	55 ± 9	43 (31−61)
PnIA	252[52]	124 (86−177)
4/3[A10L]PnIA	>10000	7900 (4200−14600)
4/4[A10L]PnIA	207 ± 66	4500 (2900−7000)
4/5[A10L]PnIA	79 ± 13	4600 (2600−8100)
4/6[A10L]PnIA	115 ± 45	3100 (2300−4100)

similarly to conotoxin 4/3[A10L]PnIA, also failing to inhibit the ACh-evoked current amplitude at concentrations up to 10 μM (Supporting Information Figure 2).

CD Analysis. CD spectra in aqueous solution were acquired for all samples, and only 4/6[A10L]PnIA maintained a helical content similar to 4/7[A10L]PnIA; all of the other truncated analogues gave CD spectra indicative of random coil structure (see Figure 4, black curves). The use of TFE as cosolvent produced different results for 4/4 and 4/5[A10L]PnIA. Specifically, the CD spectra of 4/4 and 4/5[A10L]PnIA (Figure 4) indicated that the structure changes from random coil to a more helical structure as the concentration of TFE increases (0−30%). On the other hand, 4/6 and 4/3[A10L]PnIA show very little structural change in 20−30% TFE compared to aqueous solution, being mainly a full helical structure and a random coil, respectively. CD analysis shows that 4/3[P7R, A10L]PnIA has a similar random coil structure in both aqueous and TFE organic solution as 4/3[A10L]PnIA (Supporting Information Figure 3).

NMR Analysis. NMR spectra were recorded for all analogues, and an analysis of chemical shifts showed that in aqueous solution 4/6[A10L]PnIA maintained the overall fold of [A10L]PnIA.[31] By contrast, the 4/5, 4/4, and 4/3 derivatives showed the presence of multiple conformations in aqueous solution. The peaks for the major conformations were assigned for all of the analogues except for 4/4[A10L]PnIA, which displays broad peaks in the NMR spectra. A comparison of the αH chemical shifts for the 4/7, 4/6, 4/5, and 4/3 analogues in aqueous solution is given in Figure 5A. The chemical shifts of 4/6[A10L]PnIA are very close to the native [A10L]PnIA, whereas 4/3 and 4/5[A10L]PnIA differ, suggesting an alternative conformation. The position 7 mutant 4/3[P7R, A10L]PnIA has an αH chemical shift profile similar to conotoxin 4/3[A10L]PnIA but distinct from native [A10L]PnIA (Supporting Information Figure 4). Given the influence of TFE on the CD spectra of 4/4 and 4/5[A10L]PnIA, NMR spectra were also recorded in 25% TFE. In the presence of TFE the resonances of 4/4[A10L]PnIA sharpened relative to those in spectra recorded in aqueous solution, but limited NOEs were observed, preventing a complete assignment. A native-like conformation was stabilized for 4/5[A10L]PnIA in the presence of TFE as shown in Figure 5B where the αH chemical shifts are very similar to the native peptide. The major changes occur for residues 2, 5, 7, and 8, three of which are in the reported helical region of the native peptide (residues 5−12).

Stability Experiments in Reducing Thiols. To evaluate the stability of the globular disulfide bond framework[32] with different loop sizes, we conducted stability experiments to assess the scrambling rates of the truncated analogues in reduced glutathione. Incubation of 500 μM truncated peptides with 1 equiv of glutathione showed that scrambling of the disulfide

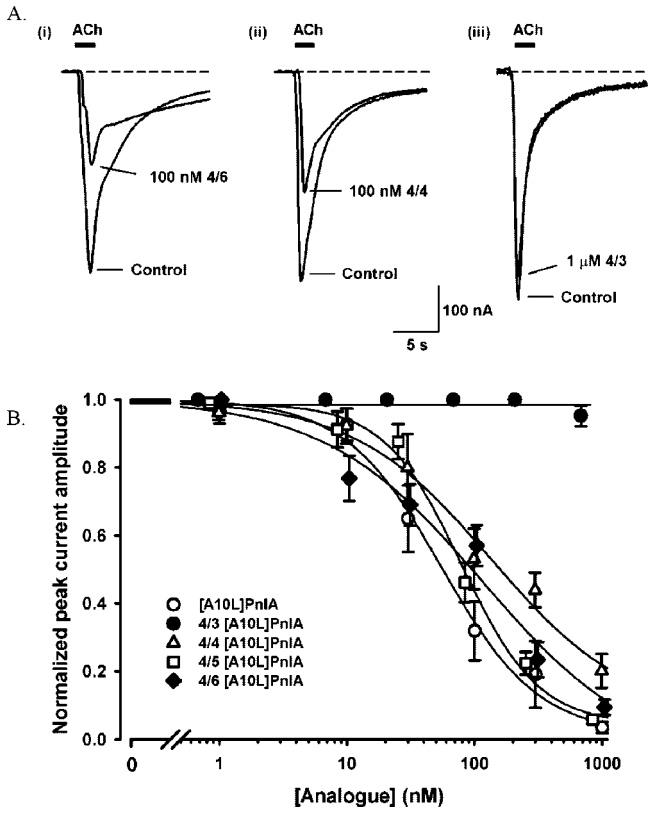

Figure 3. Effect of α-conotoxin [A10L]PnIA truncation on inhibition of rat α7 nAChRs expressed in *Xenopus* oocytes. (A) Superimposed α7 nAChR-mediated currents evoked with 200 μM ACh in the absence (control) and presence of the truncated [A10L]PnIA analogues: (i) 100 nM 4/6[A10L]PnIA, (ii) 100 nM 4/4[A10L]PnIA, and (iii) 1 μM 4/3[A10L]PnIA, respectively. (B) Concentration−response curves obtained with oocytes voltage clamped at −80 mV evoked with 200 μM ACh following a 200 s incubation of [A10L]PnIA (○), 4/3[A10L]PnIA (●), 4/4[A10L]PnIA (△), 4/5[A10L]PnIA (□), and 4/6[A10L]PnIA (◆). Data are the mean ± SEM, with the concentration−response curve for the antagonists fitted using a logistic equation (see Experimental Section).

bond framework occurs for [A10L]PnIA and its truncated analogues. HPLC analysis revealed that [A10L]PnIA and 4/6[A10L]PnIA maintained ∼40% of their native globular conformation at 8 h, whereas 4/5, 4/4, and 4/3[A10L]PnIA lost >80% of their original globular conformation within 2 h. Figure 6A shows the time-course HPLC profiles of truncated [A10L]PnIA in reduced glutathione system. Figure 6B shows the scrambling curves of truncated [A10L]PnIA peptides. Scrambling curves were generated from the height of remaining globular conformation peptides on HPLC. The results show that the half-lives for globular 4/7 and 4/6[A10L]PnIA in free thiols are about 2 h, while the half-lives for the globular 4/5, 4/4, and 4/3[A10L]PnIA are less than 30 min. Interestingly, when globular 4/3[P7R, A10L]PnIA was incubated with the reduced glutathione, it was able to maintain about 40% globular conformation after 24 h in free thiols (see Figure 6C) and its half-life is prolonged to 1 h.

AChBP Binding Assay. We measured the affinity of truncated [A10L]PnIA analogues on AChBP from *Lymnaea stagnalis* (Ls-AChBP) in a competitive binding assay with iodine-125 labeled α-bungarotoxin (^{125}I-Bgt). Surprisingly, all the truncated analogues were able to displace ^{125}I-Bgt bound to Ls-AChBP (Figure 7A). However, whereas the 4/7[A10L]PnIA displayed a K_i of 43 nM, the truncated 4/6, 4/5, 4/4, and 4/3[A10L]PnIA were all about 100-fold less potent, with K_i values of 3.1, 4.6, 4.5, and 7.9 μM, respectively. In comparison with native PnIA, conotoxin 4/7[A10L]PnIA was ∼3-fold more potent on Ls-AChBP (Table 3). Even though the truncated 4/6, 4/5, 4/4, and 4/3 displayed a similar weak micromolar activity on Ls-AChBP, a decreasing order of potency by the sequential truncation was revealed (i.e., 4/6 > 4/5 = 4/4 > 4/3).

Structural Models of PnIA and [A10L]PnIA Analogues Interactions with α7 nAChR and Ls-AChBP. Inspection of the structural alignment of the truncated analogue models with the crystal structures of [A10L, D14K]PnIA[23] (PDB ID 2BR8) and PnIA[24] (PDB ID 1PEN) suggests that the main α-helical backbone (residues 5−11) has not been altered by C-terminal truncation except for 4/3[A10L]PnIA, which contains only random coil structure after energy minimization. Subsequently the native PnIA, [A10L]PnIA, and the truncated [A10L]PnIA analogues were docked onto the model structures of α7 nAChR and Ls-AChBP individually (Figure 7B). All the analogues shared similar binding orientations and geometry in the hydrophobic aromatic pocket of α7 nAChR (Supporting Information Figure 5, parts i and ii). In contrast, [A10L]PnIA (colored in light-magenta) and 4/4[A10L]PnIA (colored in cyan) binding to Ls-AChBP was tilted by 20° around Leu5 with respect to PnIA (Supporting Information Figure 5, parts iii and iv). Our predicted binding pocket is consistent with the previous studies indicating that hydrophobic interactions are the dominant contributors to the binding of [A10L]PnIA.[23,29] The docking experiments revealed a conserved hydrogen bond between residue Asn11 in all PnIA analogues (except 4/3[A10L]PnIA) and Glu192 of the rat α7 nAChR. Interestingly, this hydrogen bond was not apparent when the truncated analogues (4/6, 4/4, 4/5, and 4/3[A10L]PnIA) were docked to Ls-AChBP. Additional hydrogen bonds were observed between Asn12 of PnIA and [A10L]PnIA and Glu190 of Ls-AChBP (Figure 7B) and between Asn11 of [A10L]PnIA and Glu149 of Ls-AChBP (Figure 7B).

Discussion

Significant advances have been achieved in the past decade in understanding the interactions between small neuronal nicotinic antagonists (α-conotoxins) and neuronal nAChR subtypes at the molecular level.[2] Although a diverse range of α-conotoxins act on neuronal nAChRs, most contain a relatively conserved first loop with a similar backbone structure in addition to a key interacting residue from the second loop with its side chain exposed on the surface of the helical α-conotoxin structure. This is reflected in the various structure−activity models proposed for individual neuronal α-conotoxins from alanine scanning mutagenesis and position scanning mutagenesis studies.[21−23,29] For instance, studies on α-conotoxin ImI have revealed that the important binding residues are D5, P6, and R7 in the first loop and W10 in the second loop.[33] For both α-conotoxins ImI and PnIB, the common crucial residues are residues 6 and 7 in the first loop and residue 10 in the second loop.[21] In contrast, α-conotoxin MII with a 4/7 loop helical structure and homologous residues to the α7-preferring conotoxin PnIB at positions 6, 7, and 10 (P6, V7, and L10) has its key binding determinants somewhat displaced at residues D5, P6, and H12[27,34] perhaps reflecting a different receptor preference. Given the above structure−function relationships of the α7-preferring conotoxins ImI and PnIB and [A10L]PnIA, we took the approach that selected α-conotoxins of the 4/7 class (e.g., [A10L]PnIA) that target the α7 nAChR may be amenable to further engineering through a pruning strategy.[30] Such a strategy would involve truncation of the larger second loop from seven to three residues (i.e., similar size to α-conotoxin ImI) and if successful would maintain full potency.

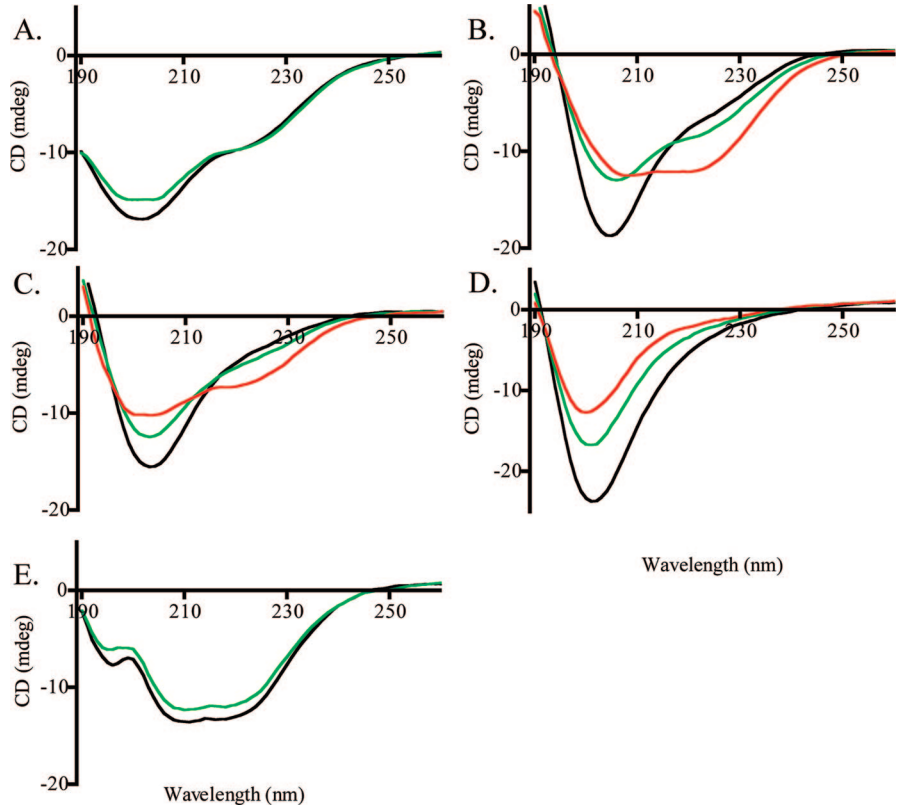

Figure 4. CD spectra of truncated [A10L]PnIA analogues at various concentrations of TFE: (A) 4/6[A10L]PnIA, (B) 4/5[A10L]PnIA, (C) 4/4[A10L]PnIA, (D) 4/3[A10L]PnIA, and (E) 4/7[A10L]PnIA. Black, green, and red curves represent 0%, 20%, and 30% TFE (v/v) at room temperature, respectively.

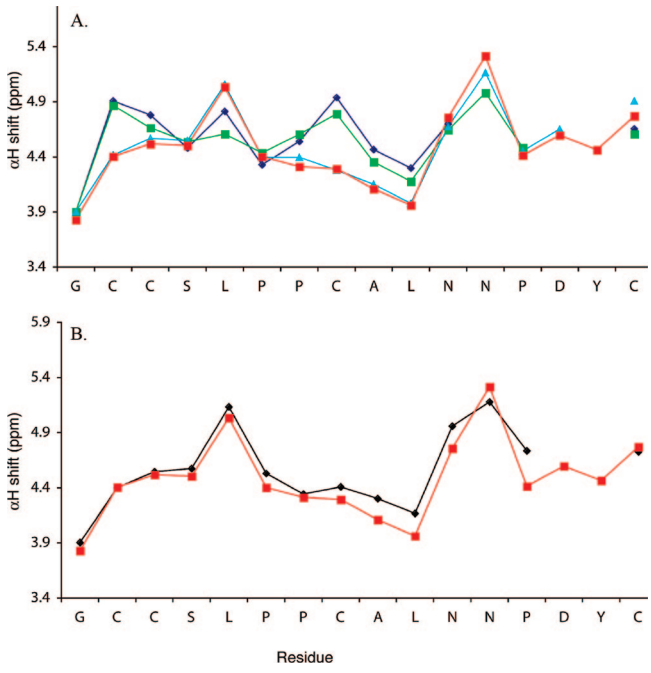

Figure 5. Chemical shift comparison of truncated [A10L]PnIA analogues: (A) aqueous solution and (B) 25% TFE. αH shifts in aqueous solution are shown as [A10L]PnIA (red square),[31] 4/6[A10L]PnIA (blue triangle), 4/5[A10L]PnIA (green square), and 4/3[A10L]PnIA (blue diamond) in the upper panel, and αH shifts in 25% TFE are shown as [A10L]PnIA (red square)[31] and 4/5[A10L]PnIA (black diamond) in the lower panel.

α-Conotoxin [A10L]PnIA is the most potent α7 nAChR ligand known with well-defined structural and functional determinants.[10,21−23] With a 4/7 loop size, this α-conotoxin provided an ideal template to investigate the role of loop size on the structural integrity and function of α-conotoxins. Truncated analogues of [A10L]PnIA with 4/6, 4/5, 4/4, and 4/3 loop sizes (Table 2) were selectively synthesized in their active globular conformation (i.e., 1−3, 2−4 cysteine connectivity) and their NMR and CD spectra used to determine their helical content and their structural integrity. The activity of each analogue was determined by electrophysiological evaluation at the rat α7 nAChR expressed in *Xenopus* oocytes.

Application of our pruning strategy provided significant insights into the structure−function relationship of α-conotoxin [A10L]PnIA at the α7 nAChR. Because hydrophobic interactions have been established as the dominant contributions to the affinity of [A10L]PnIA at α7 nAChRs,[21,23] we anticipated that the removal of the last three residues via truncation may not impact adversely on α7 nAChR ligand affinity. Thus, removal of the loop 2 remote residue Tyr15 did not affect potency, 4/6, 4/5, and 4/4 [A10L]PnIA analogues blocking the α7 nAChR at similar nanomolar levels. Indeed, when the only charged residue Asp14 was removed from the sequences of 4/5 and 4/4[A10L]PnIA, their activity was only marginally altered. Further, even though Pro13 showed critical contact in the bound Ac-AChBP crystal structure[23] and on an α7 nAChR model,[29] omitting this residue did not change the activity of 4/4[A10L]PnIA at the expressed α7 nAChR. The overall results support the mutagenesis studies from Quiram et al.[21] and are consistent with our hypothesis that smaller loop sizes are capable of maintaining nAChR activity. It is perhaps surprising to observe the almost complete loss of activity of the α-conotoxin 4/3[A10L]PnIA though the structural results described below go some way to explain this observation.

From the summary of the impact of loop size on globular structure from CD and NMR analysis (Table 4), it is clear that

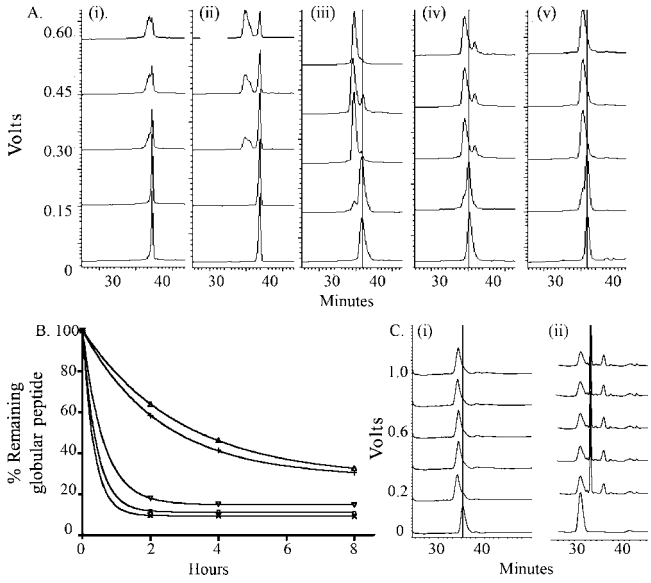

Figure 6. Disulfide bonds scrambling analysis of truncated [A10L]PnIA peptides. (A) Time-course RP-HPLC analysis of (i) [A10L]PnIA, (ii) 4/6[A10L]PnIA, (iii) 4/5[A10L]PnIA, (iv) 4/4[A10L]PnIA, and (v) 4/3[A10L]PnIA. Bottom to top HPLC traces are 0 h, 5 min, 2 h, 4 h, and 8 h, respectively. Cursors indicate where the globular isomers elute. (B) Scrambling curves of [A10L]PnIA (+), 4/6[A10L]PnIA (△), 4/5[A10L]PnIA (▽), 4/4[A10L]PnIA (×), and 4/3[A10L]PnIA (○). Curves were generated from the height of remaining globular conformation peptide on HPLC. (C) Time-course RP-HPLC analysis of globular (i) 4/3[A10L]PnIA and (ii) 4/3[P7R, A10L]PnIA peptides. Bottom to top HPLC traces are 0 h, 1 h, 2 h, 4 h, 8 h, and 24 h, respectively. Cursors indicate where the globular isomers elute.

the systematic loop truncation results in a successive loss of helical structure. Although both α-conotoxins 4/6[A10L]PnIA and 4/7[A10L]PnIA maintain full helical structure and full activity at the α7 nAChRs, significant structural heterogeneity in the analogues with smaller loop sizes (i.e., 4/5 and 4/4) was observed by NMR analysis. However, the propensity of α-conotoxins 4/5[A10L]PnIA and 4/4[A10L]PnIA to form a native-like helical structure in 20−30% TFE together with their significant activity at the α7 nAChR suggests that these heterogeneous isomers were able to adopt the active conformation at the receptor and consequently maintain activity. In contrast, α-conotoxin 4/3[A10L]PnIA is both unable to achieve a helical structure and is inactive at the α7 nAChR. It would appear that if a helical structure cannot be achieved, even as a minor conformer, then activity cannot be maintained. This deduction was supported by the inactivity of the similarly nonhelical 4/3[P7R, A10L]PnIA on the rat α7 nAChRs. The inability of globular α-conotoxin 4/3[A10L]PnIA to maintain a helical structure contrasts strongly with the potent α7-preferring conotoxin ImI, which has helical structure in both NMR[35] and bound X-ray structures.[28] Comparison of the sequences of ImI with 4/3[A10L]PnIA highlights the differences in polarity between these conotoxins with ImI containing basic residues in both loops (Arg7 and Arg12) and an acidic residue (Asp5) in the first loop as opposed to the neutral 4/3[A10L]PnIA. It has been suggested that Asp5 functions as an N-cap through side chain and backbone hydrogen bonds to stabilize the 3_{10}-helical turn forming from Pro6 to Cys8.[35] By contrast in α-conotoxin 4/3[A10L]PnIA, the hydrophobic residue Leu5 replaces the hydrophilic Asp5 found in ImI, and consequently 4/3[A10L]PnIA may lose the ability to assist helix formation through a critical hydrogen bond.

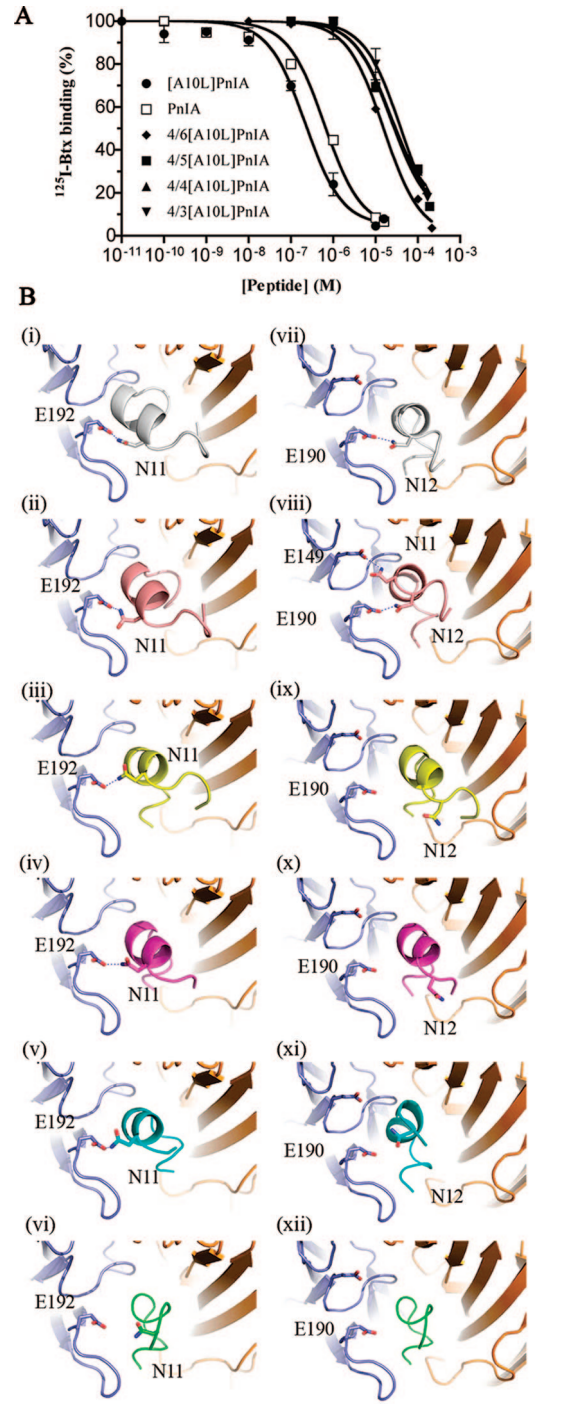

Figure 7. Effect of α-conotoxin [A10L]PnIA truncation on Ls-AChBP affinity and docking simulations. (A) Displacement of ^{125}I-Bgt from Ls-AChBP by [A10L]PnIA analogues. The data were normalized and fitted to a sigmoidal dose−response curve (slope of −1), and the K_i was calculated from the observed EC_{50} using GraphPad Prism software. (B) Comparison of the truncated PnIA analogue binding mode at α7 nAChR (left column) and Ls-AChBP (right column) ligand binding domain. The docking molecules in the left column from the top to bottom are (i) PnIA, (ii) 4/7[A10L]PnIA, (iii) 4/6[A10L]PnIA, (iv) 4/5[A10L]PnIA, (v) 4/4[A10L]PnIA, and (vi) 4/3[A10L]PnIA. A conserved hydrogen bond between Glu192 of α7 nAChR and Asn11 of the conotoxin analogues is shown as a blue dot line in all analogues except for 4/3[A10L]PnIA. The right column from the top to bottom are (vii) PnIA, (viii) 4/7[A10L]PnIA, (ix) 4/6[A10L]PnIA, (x) 4/5[A10L]PnIA, (xi) 4/4[A10L]PnIA, and (vii) 4/3[A10L]PnIA. A hydrogen bond between Asn12 of PnIA analogues and Glu190 of Ls-AChBP was identified only to PnIA and [A10]PnIA. An additional hydrogen bond between Asn11 of [A10L]PnIA and Glu49 of Ls-AChBP was also identified in part viii.

Table 4. Impact of Loop Size on Structure Determined by NMR and CD[a]

		helical content			
		CD structure		NMR structure	
framework	name	aqueous	TFE/H_2O	aqueous	TFE/H_2O
[4/7]globular	[A10L]PnIA	full helix	full helix	full helix	full helix
[4/6]globular	4/6[A10L]PnIA	full helix	full helix	full helix	full helix
[4/5]globular	4/5[A10L]PnIA	random coil	full helix	multiple conformers	full helix
[4/4]globular	4/4[A10L]PnIA	random coil	portion of helix	multiple conformers	unidentified
[4/3]globular	4/3[A10L]PnIA	random coil	random coil	multiple conformers	nd

[a] nd: not determined.

The above suggestion is consistent with our docking models, where 4/3[A10L]PnIA was found to be the only PnIA analogue that contains no α-helical structure and fails to form a hydrogen bond between Asn11 of the conotoxin and Glu192 of α7 nAChR (Figure 7B). The role of Asn12 is now proposed to maintain the PnIA analogues in the correct binding orientation such that Asn11 is able to form a hydrogen bond with α7 nAChR. A combination of AChBP binding and docking experiments provided further insights into the nature of the interactions of each residue of [A10L]PnIA with AChBP. In agreement with our previous observations,[36] [A10L]PnIA displayed stronger binding affinity than conotoxin PnIA at Ls-AChBP. In part this may reflect the presence of an additional hydrogen bond between Asn11 of [A10L]PnIA and Glu149 of Ls-AChBP, which is absent in PnIA. More striking is the 100-fold loss of potency on "pruning" 4/7 [A10L]PnIA to 4/6[A10L]PnIA through removal of Tyr15, while further deletions of Asp14 and Pro13 had minor effects on affinity to Ls-AChBP (Table 3), indicating the possibility that Tyr15 may interact directly with Ls-AChBP. However, studies of [Y15A]PnIB[21] displacement of ^{125}I-Bgt from human α7 nACh/5-HT receptors indicated that Tyr15 had little influence on affinity and thus likely lay outside the α-conotoxin binding site. Our docking models demonstrated that the binding constraints of Ls-AChBP are more flexible than α7 nAChR, as the truncated [A10L]PnIA analogues docked in different orientations in the Ls-AChBP binding pocket (20° tilted with respect to PnIA), whereas the truncated analogues are found to be in a more confined orientation (<5° difference in tilt) at α7 nAChR (Supporting Information Figure 5). These shifts in binding orientation suggest that Ls-AChBP may provide a number of alternative sets of binding interactions, whereas binding interactions at the α7 nAChR appear more specific. This hypothesis is in agreement with the cocrystal structure of [A10L, D14K]PnIA and Ac-AChBP,[23] which revealed more interactions between the conotoxin and the Ac-AChBP receptor than was suggested from the mutagenesis study (Table 1). The sequential pruning of the second loop of [A10L]PnIA led to decreased binding affinity to Ls-AChBP, which confirmed the interactions previously observed from the cocrystal structure of [A10L, D14K]PnIA and AChBP. The reduced potency was also supported by our Ls-AChBP docking models that reveal that an important hydrogen bond interaction between Asn12 of the conotoxin and Glu190 of Ls-AChBP is lost in all truncated analogues. The fact that 4/3[A10L]PnIA maintained weak affinity at Ls-AChBP but not at the α7 nAChR supports our hypothesis that more interactions are accessible to α-conotoxins binding to Ls-AChBP than to α7 nAChR. Apparently the loss of the Asn12 hydrogen bond in the 4/3[A10L]PnIA Ls-AChBP binding interaction can be compensated by interactions within in the binding pocket.

The observation that the 4/6, 4/5, and 4/4[A10L]PnIA analogues are potent at the rat α7 nAChR but exhibit 100-fold lower affinity at the molluscan Ls-AChBP is not without precedent. This phenomenon has been observed previously with α-conotoxin ImI and TxIA. Conotoxin ImI shows high potency at the rat α7 nAChR (IC_{50} = 132 nM)[28] but very low affinity at the molluscan Ls-AChBP (K_i = 14 000 nM).[37] In contrast, TxIA showed high affinity to molluscan Ls-AChBP (K_i = 1.7 nM) but 200-fold less potency toward the α7 nAChR (IC_{50} = 392 nM).[36]

An interesting observation was the significant broadening of peaks in the NMR spectra of 4/4[A10L]PnIA despite maintenance of almost full activity. This is consistent with the NMR structural analysis of α-conotoxin BuIA[20] where the globular 4/4 spacing does not favor a single conformation in solution. Multiple sets of peaks were observed in the NMR spectra of globular BuIA, indicative of at lease three conformers in slow exchange on the NMR time scale. The broadening observed in the NMR spectra of 4/4[A10L]PnIA indicates intermediate exchange between at least two conformers.

Disulfide bonds are kinetically unstable in thiol-containing environments,[38,39] and the scrambling rate by thiol-containing molecules such as glutathione or serum albumin can be used to evaluate the stability of α-conotoxin disulfide bond frameworks.[32] We anticipated that truncation of an already constrained disulfide bond framework may lead to increased strain and consequently increased susceptibility to thiol interchange. This was indeed observed with a dramatic decrease of stability for the 4/5, 4/4, and 4/3[A10L]PnIA globular frameworks when compared with α-conotoxins 4/7 and 4/6[A10L]PnIA. The fact that the half-life of globular 4/3[A10L]PnIA is only 17 min in comparison with the naturally occurring globular 4/3 ImI, which has a 2 h half-life[32] in the presence of free thiol, is consistent with the induced strain hypothesis. Such strain may derive more from the specific sequence differences (four residues different), as both α-conotoxins ImI and [A10L]PnIA maintain the conserved Pro6 and Ser4 residues found in the first loop of most α-conotoxins. It is also conceivable that preservation of Pro6Pro7 in the first loop of globular 4/3[A10L]PnIA may have restricted this analogue from achieving conformational stability. On the basis of these assumptions, α-conotoxin 4/3[P7R, A10L]PnIA was prepared with the globular disulfide bond connectivity in which arginine was used to replace Pro7, thus mimicking positions 6 and 7 in α-conotoxin ImI. With a change of a single residue in α-conotoxin 4/3[A10L]PnIA, the half-life of 4/3[P7R, A10L]PnIA in the presence of free thiols was increased to 1 h. Though the single residue change was insufficient to give a defined structure, it clearly helped release strain in this truncated analogue.

Disulfide bond frameworks constitute essential structural elements in α-conotoxins, and stabilizing such frameworks is also a key factor in their small molecule design and development. In order to avoid the "penalty" of decreased conformational stability, future efforts will introduce selenocysteine residues into the engineered α-conotoxin frameworks, as diselenide bonds are kinetically more stable than disulfide bonds.[40] The selenocystine strategy has been applied successfully in

stabilizing the framework of α-conotoxin ImI[32] where full activity and a highly stable isomorphic structure were obtained.

Conclusions

This is the first study that demonstrates that it is possible to progressively truncate loop 2 of a two-loop containing α-conotoxin (4/7 class) while maintaining full potency. Through molecular engineering studies of [A10L]PnIA it appears that neither a 4/7 framework nor a pre-existing helical structure is necessary for full potency of [A10L]PnIA at the α7 nAChRs. However, the penalty for these "pruned" versions of [A10L]PnIA is decreased conformational stability, as reflected by the presence of multiple conformations in solution and faster scrambling rates of the small loop sized truncated analogues in a reducing environment. This novel engineering strategy sheds further insights into the structure−function relationships of the α-conotoxins, including a requirement for loops 1 and 2 complementarity for helical stability. These results are supported by docking simulations which can help guide future attempts to develop potent peptide mimetics of the α-conotoxins.

Experimental Section

Materials. *N*-α-Boc-L-amino acids and reagents used for peptide chain assembly were peptide synthesis grade purchased from NovaBiochem (San Diego, CA). 4-Methylbenzhydrylamine resin was purchased from Peptide Institute (Osaka, Japan). *p*-Cresol and *p*-thiocresol were purchased from Aldrich (Sydney, Australia). HBTU was purchased from Richelieu Biotechnologies (Quebec, Canada). Screw-cap glass peptide synthesis reaction vessels with sintered glass filter frit were obtained from Embell Scientific glassware (Queensland, Australia). Anhydrous HF was purchased from Matheson Gas (BOC Gases, Melbourne, Australia). All of the solvents used for HPLC and peptide synthesis were purchased from Labscan (Bangkok, Thailand). Water measuring 18.2 MΩ was from ELGA system (Melbourne, Australia).

Peptide Synthesis. Assembly of the truncated [A10L]PnIA [4/3, 4/4, 4/5, 4/6] analogues, as well as 4/3[P7R, A10L]PnIA, was performed manually using the stepwise *in situ* neutralization protocol for Boc chemistry.[41] The four cysteine residues were differentially protected with HF-labile methylbenzyl groups (CysII and CysIV) and HF-resistant acetamidomethyl groups (CysI and CysIII). Other amino acid side chain protection was as follows: Tyr (BrZ), Asn (Xan), Asp (OcHex), and Ser (Bzl). All the syntheses were carried out on a 0.5 mmol scale using HBTU (0.5 M/DMF) as the activation reagent and DIEA as neutralizing reagent on 4-methylbenzhydrylamine (MBHA) resin. Neat TFA was used as the amine-deprotecting reagent. The coupling efficiencies were determined using the quantitative ninhydrin test.[42] Double coupling was applied when the first coupling efficiency was less than 99%, as well as after each proline residue. Following the assembly, ∼300 mg of resin for each peptide was cleaved by 10 mL of HF/*p*-cresol/*p*-thiocresol (18:1:1) at 0 °C for 120 min. After the cleavage, HF was evaporated, and all peptides were precipitated and washed by cold diethyl ether (50 mL × 3). The crude peptides were dissolved in 45% acetonitrile/0.05%TFA/H_2O and lyophilized. The crude linear peptide was identified by MS and purified by HPLC. 4-Methylbenzyl groups attached to cysteines were removed during the HF cleavage, and the oxidation of the first disulfide bond was performed in 0.1 M NH_4HCO_3 oxidation buffer at pH 8 at a concentration of 0.1 mg/mL. The one pair disulfide-bonded peptides were purified by HPLC and lyophilized prior to the formation of the second disulfide bond. Simultaneous deprotection and oxidation of Acm protected cysteine residues were performed in 80% methanol at pH 2−3. The peptide concentration in this reaction was 0.2 mg/mL, 1 M HCl adjusted the pH, and 10-fold iodine (0.1 M in MeOH) was added. The reaction mixture was stirred for 5 min under argon. Methanol and iodine were evaporated via rotary evaporation. The resultant mixture was diluted 100-fold by MQ-H_2O and purified by HPLC.

RP-HPLC and Mass Spectrometry. Preparative HPLC was performed on Waters 600E solvent delivery system. Data were collected via a 484-absorbance detector from Waters at 230 nm. Analytical HPLC was performed on Shimadzu LC-2010 instruments. Preparative HPLC was carried out using a Phenomenex C_{18} column (250 mm × 21.20 mm, 10 μm). Analytical HPLC was performed on a Phenomenex C_{18} (250 mm × 4.6 mm, 10 μm) column. 90% acetonitrile and 0.043% trifluoroacetic acid were used as the eluting buffer B. 0.05% trifluoroacetic acid was used as the eluting buffer A. 1% B per minute was used as the linear gradient at standard column flow rates (8 mL/min for preparative HPLC and 1 mL/min for analytical HPLC). Electrospray mass spectra were acquired on a Micromass LCT (Manchester, U.K.), a liquid chromatography orthogonal acceleration reflecting TOF mass spectrometer coupled to an Agilent HPLC system. Samples (∼5 μL) were injected into a moving solvent (70 μL/min, 70% acetonitrile/0.05% formic acid/H_2O) coupled directly to the electrospray ionization source. Full scan mass spectra were acquired over the mass range of 400−1600 Da with a scan step size of 0.2 Da. Molecular masses were derived from the observed *m*/*z* values.

Functional Characterization. RNA was prepared from cDNA encoding the rat α7 nAChR subunit (provided by J. Patrick, Baylor College of Medicine, Houston, TX). *Xenopus laevis* were then anesthetized using tricaine methane sulfonate (1.5 g/L) and oocytes surgically removed before being placed in OR-2 buffer (82.5 mM NaCl, 2 mM KCl, 1 mM $MgCl_2$, and 5 mM HEPES at pH 7.4) with 3 mg/mL collagenase (Sigma) for 1−2 h at room temperature. Collagenase was removed by further rinsing 3 times in the same OR-2 solution at 18 °C, followed by a further 3 rinses in the final ND96 buffer (96 mM NaCl, 2 mM KCl, 1.8 mM $CaCl_2$, 1 mM $MgCl_2$, and 5 mM HEPES at pH 7.5) supplemented with 50 mg/L gentamycin and 5 mM pyruvic acid. Oocytes were injected with 50 ng of cRNA and then kept at 18 °C in ND96 buffer for 2−8 days before recording.

Membrane currents were recorded from *Xenopus* oocytes using the two-electrode (virtual ground circuit) voltage clamp technique on an automated workstation with eight channels in parallel and online analysis (OpusXpress 6000A workstation, Molecular Devices, Sunnyvale, CA). Both the voltage recording and current injecting electrodes were pulled from GC150T-15 borosilicate glass (Harvard Apparatus, Edenbridge, U.K.) and filled with 3 M KCl with resistances between 0.2 and 1.5 MΩ. All recordings were conducted at room temperature (20−23 °C) using a bath solution of ND96 as described above. During recordings, the oocytes were perfused continuously at a rate of 1.5 mL/min. Acetylcholine 200 μM was applied for 2 s at 5 mL/min, with 600 s washout periods between successive applications with 200 s incubations of the [A10L]PnIA analogues. Cells were voltage-clamped at a holding potential of −80 mV. Data were sampled at 500 Hz and low pass filtered at 200 Hz. Peak current amplitude was measured before and after incubation of [A10L]PnIA analogues. All data were pooled (n = 3−10 for each data point) and represent the mean ± SEM. Concentration−response curves for antagonists were fitted by unweighted nonlinear regression to the logistic equation

$$E_x = E_{max} X^n / (X^n + IC_{50}{}^n)$$

where E_x is the response, X the antagonist concentration, E_{max} the maximal response, n the slope factor, and IC_{50} the antagonist concentration that gives 50% inhibition of the agonist response. Computation was done using SigmaPlot 8.0 (Jandel Corporation, San Rafael, CA).

CD Analysis. CD spectra were recorded on a Jasco J-810 spectropolarimeter by accumulating 10 scans obtained with a scanning speed of 50 nm/min and response of 4 s. All experiments were conducted at room temperature and monitored in the low-UV region (190−260 nm). Peptide concentration was 100 μM in sodium phosphate buffer (20 mM) at pH 7. Trifluoroethanol (TFE) induced spectra were recorded in 20% or 30% TFE in phosphate buffer (v/v). The path length of the cell was 1 mm. Helical content was judged by comparing the ellipticity of peptides at 222 nm.

NMR Spectroscopy. Samples for ^{1}H NMR measurements contained ~1 mM peptide in 90% H_2O 10% ^2H_2O (v/v) at ~pH 3. ^2H_2O (99.9% and 99.99%) was obtained from Cambridge Isotope Laboratories, Woburn, MA. Spectra were recorded at 290 K on a Bruker ARX-500 or Bruker DMX 600 spectrometer equipped with a shielded gradient unit. The 2D NMR spectra were recorded in phase-sensitive mode using time-proportional phase incrementation for quadrature detection in the t_1 dimension. The 2D experiments consisted of a TOCSY using a MLEV-17 spin lock sequence with a mixing time of 80 ms and DQF-COSY, ECOSY, and NOESY with mixing times of 250 ms. Solvent suppression was achieved using a modified WATERGATE sequence. Spectra were acquired over 6024 Hz with 4096 complex data points in F_2 and 512 increments in the F_1 dimension. Spectra were processed on a Silicon Graphics Octane workstation using XWINNMR (Bruker) software. The t_1 dimension was zero-filled to 1024 real data points, and 90° phase-shifted sine bell window functions were applied prior to Fourier transformation. Chemical shifts were referenced to internal sodium 2,2-dimethyl-2-silapentane-5-sulfonate.

Stability Experiments in Reducing Thiols. An amount of 100 μL of reduced glutathione (1 mM) in phosphate buffer (20 mM, pH 7.4) was incubated at 37 °C for 5 min. Then 100 μL of peptide solution (1 mM in 20 mM phosphate buffer, pH 7.4) was added to the glutathione solution. The vortexed reaction mixture was kept incubating at 37 °C. Aliquots of 30 μL sample were taken out of the reaction mixture at 0, 5 min, 1 h, 2 h, 4 h, 8 h, and 24 h sequentially, and the reaction was quenched immediately with 30 μL of buffer, which contains 0.5% trifluoroacetic acid. Then 50 μL of the extracted reaction mixture was injected into analytical RP-HPLC for analysis. The percentage of the remaining globular isomer was determined by measuring the peak height.

AChBP Binding Assay. The affinity of various truncated PnIA analogues relative to PnIA was determined from the displacement of ^{125}I-Bgt from Ls-AChBP following the method previously described.[43] The data were normalized and fitted to a sigmoidal dose−response curve (slope of −1), and the K_i was calculated from the observed EC_{50} using GraphPad Prism software. Experiments were performed in duplicate.

Molecular Modeling and Docking. Molecular models of truncated [A10L]PnIA analogues 4/3 and 4/4 were built using ImI[44](PDB ID 1E75) and Bu1A[45] (PDB ID 2I28) as the template, respectively, and the model of truncated analogues 4/5 and 4/6 were created using AuIB[12] (PDB ID 1MXN) as the template, with the program Modeler 9v2.[46] These templates were chosen because they share a high degree of protein sequence identities with the truncated PnIA analogues, as determined by BLAST5. To build the molecular models of the extracellular ligand binding domain of α7 nAChR, the cocrystal structure of Ac-AChBP and [A10L, D14K]PnIA[23] (PDB ID 2BR8) and the refined structure of the *Torpedo* nAChR[47] (PDB ID 2BG9) were chosen as templates, as the Ac-AChBP cocrystal structure is of higher resolution (2.4 Å) and nAChR shares higher protein sequence identity (42%, BLAST [48]). The sequence alignment was generated using ClustalW [49]and was further corrected by hand. The alignment allowed us to build models of the extracellular binding domain of α7 nAChR using the program Modeler 9v2.[46] A comparative model of Ls-AChBP was generated as described for α7 nAChR except that the Ac-AChBP cocrystal structure was the only template used. The native PnIA, [A10L]PnIA, and truncated [A10L]PnIA analogues were docked to the structures of Ls-AChBP and the extracellular ligand binding domain of α7 nAChR using the program HEX 5.0,[50] and the solutions that disagreed with the known interactions were excluded. The potential hydrogen bonds were predicted using the online server WHAT IF.[51]

Acknowledgment. This study was supported by a grant from Australian Research Council and a Program Grant from the NHMRC.

Supporting Information Available: Figures showing MS and HPLC profiles, concentration−response curves, CD spectra, chemical shift comparison, and docking models. This material is available free of charge via the Internet at http://pubs.acs.org.

References

(1) Hogg, R. C.; Raggenbass, M.; Bertrand, D. Nicotinic acetylcholine receptors: from structure to brain function. *Rev. Physiol. Biochem. Pharmacol.* **2003**, *147*, 1–46.
(2) Sine, S. M.; Engel, A. G. Recent advances in Cys-loop receptor structure and function. *Nature* **2006**, *440*, 448–455.
(3) Lloyd, G. K.; Williams, M. Neuronal nicotinic acetylcholine receptors as novel drug targets. *J. Pharmacol. Exp. Ther.* **2000**, *292*, 461–467.
(4) Gray, W. R.; Luque, A.; Olivera, B. M.; Barrett, J.; Cruz, L. J. Peptide toxins from *Conus geographus* venom. *J. Biol. Chem.* **1981**, *256*, 4734–4740.
(5) McIntosh, J. M.; Santos, A. D.; Olivera, B. M. Conus peptides targeted to specific nicotinic acetylcholine receptor subtypes. *Annu. Rev. Biochem.* **1999**, *68*, 59–88.
(6) Dutton, J. L.; Craik, D. J. α-Conotoxins: nicotinic acetylcholine receptor antagonists as pharmacological tools and potential drug leads. *Curr. Med. Chem.* **2001**, *8*, 327–344.
(7) Janes, R. W. α-Conotoxins as selective probes for nicotinic acetylcholine receptor subclasses. *Curr. Opin. Pharmacol.* **2005**, *5*, 280–292.
(8) Ellison, M.; Olivera, B. M. α4/3 Conotoxins: phylogenetic distribution, functional properties, and structure−function insights. *Chem. Rec.* **2007**, *7*, 341–353.
(9) Dutertre, S.; Nicke, A.; Lewis, R. J. Beta 2 subunit contribution of 4/7 α-conotoxin binding to the nicotinic acetylcholine receptor. *J. Biol. Chem.* **2005**, *280*, 30460–30468.
(10) Hogg, R. C.; Miranda, L. P.; Craik, D. J.; Lewis, R. J.; Alewood, P. F.; Adams, D. J. Single amino acid substitutions in α-conotoxin PnIA shift selectivity for subtypes of the mammalian neuronal nicotinic acetylcholine receptor. *J. Biol. Chem.* **1999**, *274*, 36559–36564.
(11) Quiram, P. A.; Jones, J. J.; Sine, S. M. Pairwise interactions between neuronal α7 acetylcholine receptors and α-conotoxin ImI. *J. Biol. Chem.* **1999**, *274*, 19517–19524.
(12) Dutton, J. L.; Bansal, P. S.; Hogg, R. C.; Adams, D. J.; Alewood, P. F.; Craik, D. J. A new level of conotoxin diversity, a non-native disulfide bond connectivity in α-conotoxin AuIB reduces structural definition but increases biological activity. *J. Biol. Chem.* **2002**, *277*, 48849–48857.
(13) Kaas, Q.; Westermann, J.-C.; Halai, R.; Wang, C.; Craik, D. ConoServer, a database for conopeptide sequences and structures. *Bioinformatics* **2008**, *24*, 445–446.
(14) Luo, S.; Kulak, J. M.; Cartier, G. E.; Jacobsen, R. B.; Yoshikami, D.; Olivera, B. M.; McIntosh, J. M. α-Conotoxin AuIB selectively blocks α3β4 nicotinic acetylcholine receptors and nicotine-evoked norepinephrine release. *J. Neurosci.* **1998**, *18*, 8571–8579.
(15) McIntosh, J. M.; Yoshikami, D.; Mahe, E.; Nielsen, D. B.; Rivier, J. E.; Gray, W. R.; Olivera, B. M. A nicotinic acetylcholine receptor ligand of unique specificity, α-conotoxin ImI. *J. Biol. Chem.* **1994**, *269*, 16733–16739.
(16) Ellison, M.; McIntosh, J. M.; Olivera, B. M. α-Conotoxins ImI and ImII. Similar α7 nicotinic receptor antagonists act at different sites. *J. Biol. Chem.* **2003**, *278*, 757–764.
(17) Yuan, D. D.; Han, Y. H.; Wang, C. G.; Chi, C. W. From the identification of gene organization of α-conotoxins to the cloning of novel toxins. *Toxicon* **2007**, *49*, 1135–1149.
(18) Azam, L.; Dowell, C.; Watkins, M.; Stitzel, J. A.; Olivera, B. M.; McIntosh, J. M. α-Conotoxin BuIA, a novel peptide from *Conus bullatus*, distinguishes among neuronal nicotinic acetylcholine receptors. *J. Biol. Chem.* **2005**, *280*, 80–87.
(19) Marx, U. C.; Daly, N. L.; Craik, D. J. NMR of conotoxins: structural features and an analysis of chemical shifts of post-translationally modified amino acids. *Magn. Reson. Chem.* **2006**, *44*, S41–S50.
(20) Jin, A. H.; Brandstaetter, H.; Nevin, S. T.; Tan, C. C.; Clark, R. J.; Adams, D. J.; Alewood, P. F.; Craik, D. J.; Daly, N. L. Structure of α-conotoxin BuIA: influences of disulfide connectivity on structural dynamics. *BMC Struct. Biol.* **2007**, *7*, 28.
(21) Quiram, P. A.; McIntosh, J. M.; Sine, S. M. Pairwise interactions between neuronal α7 acetylcholine receptors and α-conotoxin PnIB. *J. Biol. Chem.* **2000**, *275*, 4889–4896.
(22) Hogg, R. C.; Hopping, G.; Alewood, P. F.; Adams, D. J.; Bertrand, D. α-Conotoxins PnIA and [A10L]PnIA stabilize different states of the α7-L247T nicotinic acetylcholine receptor. *J. Biol. Chem.* **2003**, *278*, 26908–26914.
(23) Celie, P. H.; Kasheverov, I. E.; Mordvintsev, D. Y.; Hogg, R. C.; van Nierop, P.; van Elk, R.; van Rossum-Fikkert, S. E.; Zhmak, M. N.; Bertrand, D.; Tsetlin, V.; Sixma, T. K.; Smit, A. B. Crystal structure of nicotinic acetylcholine receptor homolog AChBP in complex with an α-conotoxin PnIA variant. *Nat. Struct. Mol. Biol.* **2005**, *12*, 582–588.

(24) Hu, S. H.; Gehrmann, J.; Guddat, L. W.; Alewood, P. F.; Craik, D. J.; Martin, J. L. The 1.1 Å crystal structure of the neuronal acetylcholine receptor antagonist, α-conotoxin PnIA from *Conus pennaceus*. *Structure* **1996**, *4*, 417–423.
(25) Hu, S. H.; Gehrmann, J.; Alewood, P. F.; Craik, D. J.; Martin, J. L. Crystal structure at 1.1 Å resolution of α-conotoxin PnIB: comparison with α-conotoxins PnIA and GI. *Biochemistry* **1997**, *36*, 11323–11330.
(26) Lamthanh, H.; Jegou-Matheron, C.; Servent, D.; Menez, A.; Lancelin, J. M. Minimal conformation of the α-conotoxin ImI for the α7 neuronal nicotinic acetylcholine receptor recognition: correlated CD, NMR and binding studies. *FEBS Lett.* **1999**, *454*, 293–298.
(27) Everhart, D.; Cartier, G. E.; Malhotra, A.; Gomes, A. V.; McIntosh, J. M.; Luetje, C. W. Determinants of potency on α-conotoxin MII, a peptide antagonist of neuronal nicotinic receptors. *Biochemistry* **2004**, *43*, 2732–2737.
(28) Ulens, C.; Hogg, R. C.; Celie, P. H.; Bertrand, D.; Tsetlin, V.; Smit, A. B.; Sixma, T. K. Structural determinants of selective α-conotoxin binding to a nicotinic acetylcholine receptor homolog AChBP. *Proc. Natl. Acad. Sci. U.S.A.* **2006**, *103*, 3615–3620.
(29) Dutertre, S.; Nicke, A.; Tyndall, J. D.; Lewis, R. J. Determination of α-conotoxin binding modes on neuronal nicotinic acetylcholine receptors. *J. Mol. Recognit.* **2004**, *17*, 339–347.
(30) Andrews, P.; Lloyd, E.; Martin, J.; Munro, S. Central nervous system drug design. *J. Mol. Graphics* **1986**, *4*, 41–45.
(31) Hopping, G. Synthesis, Structure and Activity of Disulfide-Rich Conus Peptides. Ph.D Thesis, Institute for Molecular Bioscience, University of Queensland, Brisbane, Australia, 2006; p 189.
(32) Armishaw, C. J.; Daly, N. L.; Nevin, S. T.; Adams, D. J.; Craik, D. J.; Alewood, P. F. α-Selenoconotoxins: a new class of potent α7 neuronal nicotinic receptor antagonists. *J. Biol. Chem.* **2006**, *281*, 14136–14143.
(33) Quiram, P. A.; Sine, S. M. Structural elements in α-conotoxin ImI essential for binding to neuronal α7 receptors. *J. Biol. Chem.* **1998**, *273*, 11007–11011.
(34) McIntosh, J. M.; Azam, L.; Staheli, S.; Dowell, C.; Lindstrom, J. M.; Kuryatov, A.; Garrett, J. E.; Marks, M. J.; Whiteaker, P. Analogs of α-conotoxin MII are selective for α6-containing nicotinic acetylcholine receptors. *Mol. Pharmacol.* **2004**, *65*, 944–952.
(35) Rogers, J. P.; Luginbuhl, P.; Shen, G. S.; McCabe, R. T.; Stevens, R. C.; Wemmer, D. E. NMR solution structure of α-conotoxin ImI and comparison to other conotoxins specific for neuronal nicotinic acetylcholine receptors. *Biochemistry* **1999**, *38*, 3874–3882.
(36) Dutertre, S.; Ulens, C.; Buttner, R.; Fish, A.; van Elk, R.; Kendel, Y.; Hopping, G.; Alewood, P. F.; Schroeder, C.; Nicke, A.; Smit, A. B.; Sixma, T. K.; Lewis, R. J. AChBP-targeted α-conotoxin correlates distinct binding orientations with nAChR subtype selectivity. *EMBO J.* **2007**, *26*, 3858–3867.
(37) Taylor, P.; Talley, T. T.; Radic, Z.; Hansen, S. B.; Hibbs, R. E.; Shi, J. Structure-guided drug design: conferring selectivity among neuronal nicotinic receptor and acetylcholine-binding protein subtypes. *Biochem. Pharmacol.* **2007**, *74*, 1164–1171.
(38) Rabenstein, D.; Weaver, K. Kinetics and equilibria of the thiol/disulfide exchange reactions of somatostatin with glutathione. *J. Org. Chem.* **1996**, *61*, 7391–7397.
(39) Hogg, P. Disulfide bonds as switches for protein function. *Trends Biochem. Sci.* **2003**, *28*, 210–214.
(40) Moroder, L. Isosteric replacement of sulfur with other chalcogens in peptides and proteins. *J. Pept. Sci.* **2005**, *11*, 187–214.
(41) Schnolzer, M.; Alewood, P.; Jones, A.; Alewood, D.; Kent, S. B. In situ neutralization in Boc-chemistry solid phase peptide synthesis. Rapid, high yield assembly of difficult sequences. *Int. J. Pept. Protein Res.* **1992**, *40*, 180–193.
(42) Sarin, V. K.; Kent, S. B.; Tam, J. P.; Merrifield, R. B. Quantitative monitoring of solid-phase peptide synthesis by the ninhydrin reaction. *Anal. Biochem.* **1981**, *117*, 147–157.
(43) Loughnan, M.; Nicke, A.; Jones, A.; Schroeder, C. I.; Nevin, S. T.; Adams, D. J.; Alewood, P. F.; Lewis, R. J. Identification of a novel class of nicotinic receptor antagonists: dimeric conotoxins VxXIIA, VxXIIB, and VxXIIC from *Conus vexillum*. *J. Biol. Chem.* **2006**, *281*, 24745–24755.
(44) Rogers, J. P.; Luginbuhl, P.; Pemberton, K.; Harty, P.; Wemmer, D. E.; Stevens, R. C. Structure−activity relationships in a peptidic α7 nicotinic acetylcholine receptor antagonist. *J. Mol. Biol.* **2000**, *304*, 911–926.
(45) Chi, S. W.; Kim, D. H.; Olivera, B. M.; McIntosh, J. M.; Han, K. H. NMR structure determination of α-conotoxin BuIA, a novel neuronal nicotinic acetylcholine receptor antagonist with an unusual 4/4 disulfide scaffold. *Biochem. Biophys. Res. Commun.* **2006**, *349*, 1228–1234.
(46) Fiser, A.; Sali, A. Modeller: generation and refinement of homology-based protein structure models. *Methods Enzymol.* **2003**, *374*, 461–491.
(47) Unwin, N. Refined structure of the nicotinic acetylcholine receptor at 4 Å resolution. *J. Mol. Biol.* **2005**, *346*, 967–989.
(48) Altschul, S. F.; Gish, W.; Miller, W.; Myers, E. W.; Lipman, D. J. Basic local alignment search tool. *J. Mol. Biol.* **1990**, *215*, 403–410.
(49) Larkin, M. A.; Blackshields, G.; Brown, N. P.; Chenna, R.; McGettigan, P. A.; McWilliam, H.; Valentin, F.; Wallace, I. M.; Wilm, A.; Lopez, R.; Thompson, J. D.; Gibson, T. J.; Higgins, D. G. Clustal W and Clustal X version 2.0. *Bioinformatics* **2007**, *23*, 2947–2948.
(50) Ritchie, D. W.; Kemp, G. J. Modelling antibody side chain conformations using heuristic database search. *Proc. Int. Conf. Intell. Syst. Mol. Biol.* **1997**, *5*, 237–240.
(51) Vriend, G. WHAT IF: a molecular modeling and drug design program. *J. Mol. Graphics* **1990**, *8*, 52–56.
(52) Luo, S.; Nguyen, T. A.; Cartier, G. E.; Olivera, B. M.; Yoshikami, D.; McIntosh, J. M. Single-residue alteration in α-conotoxin PnIA switches its nAChR subtype selectivity. *Biochemistry* **1999**, *38*, 14542–14548.

JM800278K